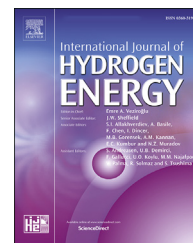


Available online at [www.sciencedirect.com](http://www.sciencedirect.com)

ScienceDirect

journal homepage: [www.elsevier.com/locate/he](http://www.elsevier.com/locate/he)

## Short Communication

## Metal loading effects on carbon-supported Pd electrocatalysts



E.G. Ciapina <sup>a,\*</sup>, L.B. Viana <sup>a</sup>, R.M.I.S. Santos <sup>a</sup>, M.S.M. Nogueira <sup>a</sup>,  
O.P. Almeida-Júnior <sup>a</sup>, R.S. Nunes <sup>a</sup>, S.F. Santos <sup>b</sup>, R.Z. Nakazato <sup>a</sup>

<sup>a</sup> São Paulo State University (Unesp) – School of Engineering, Guaratinguetá, São Paulo, Brazil

<sup>b</sup> Centro de Engenharia, Modelagem e Ciências Sociais Aplicadas – UFABC, Av. Dos Estados 5001, 09210-580, Santo André, São Paulo, Brazil

## ARTICLE INFO

## Article history:

Received 20 November 2017

Received in revised form

26 March 2018

Accepted 21 July 2018

Available online 16 August 2018

## Keywords:

Palladium

Metal loading

Electrocatalysts

Cyclic voltammetry

Carbon

## ABSTRACT

We report for the first time effects of altering the amount of Pd supported on high-surface area carbon (Pd/C). Cyclic voltammetry in 0.1 M H<sub>2</sub>SO<sub>4</sub> using Pd/C electrocatalysts with distinct metal-to-carbon ratio, Pd black and a Pd wire electrodes reveals unambiguously metal loading effects, such as a decrease in the peak potential for the reduction of palladium oxide (PdO), an increase of the charges of desorption of hydrogen, and formation/reduction of PdO with the Pd content. Such effects need to be taken into account when designing Pd-based Fuel Cells electrocatalysts.

© 2018 Hydrogen Energy Publications LLC. Published by Elsevier Ltd. All rights reserved.

## Introduction

Carbon-supported palladium nanoparticles (Pd/C) has been considered as a potential substitute for Platinum-based electrocatalysts in Direct Formate Fuel Cells and Direct Formic Acid Fuel Cells, as described in detail in some reviews [1–3].

Despite the several studies showing its catalytic activity towards the electrochemical oxidation of formic acid/formate [4–6], ethanol [7–9] and also for the reduction of molecular oxygen (oxygen reduction reaction, ORR) [10–12], it is surprising that very little attention has been given to the

fundamental electrochemical behavior of carbon-supported Pd-containing materials in the absence of any electro-active species, that is, solely in the supporting electrolyte.

With respect to supported metal electrocatalysts, studies mainly carried out with Pt-based materials have shown that several parameters may, in principle, affect the overall observed electrochemical response, such as size, morphology, and loading of the metal crystallites onto the support phase [13–18]. However, due to the lack of a detailed study in the literature regarding the behavior of nano-sized Pd particles anchored in high surface area carbon, we decided to

\* Corresponding author.

E-mail address: [eduardociapina@feg.unesp.br](mailto:eduardociapina@feg.unesp.br) (E.G. Ciapina).

<https://doi.org/10.1016/j.ijhydene.2018.07.137>

0360-3199/© 2018 Hydrogen Energy Publications LLC. Published by Elsevier Ltd. All rights reserved.

investigate the effect of the metal loading on current-potential characteristics of Pd/C electrocatalysts by cyclic voltammetry. By keeping the same preparation procedure, it was synthesized Pd/C samples with distinct amounts of Pd anchored on carbon. Herein, we will show for the first time that the amount of Pd loaded on carbon results in significant changes in the cyclic voltammetric behavior, clearly exhibiting metal loading effects.

## Experimental

Pd nanoparticles were prepared by a similar method described by Lima et al. [19]. Briefly, the procedure is based on the reduction of an aqueous solution of  $\text{PdCl}_2$  (Sigma-Aldrich) by excess of aqueous  $\text{NaBH}_4$  (Sigma-Aldrich) in the presence sodium citrate (Sigma-Aldrich). Adequate amounts of high surface area carbon (Vulcan XC-72R, Cabot Co.) previously suspended in ultra-pure water were added to obtain the desired metal-to-carbon ratio. All reagents were used as received with the exception of the high-surface area carbon, treated with diluted  $\text{HNO}_3$  for 12 h and washed thoroughly several times with deionized water to remove possible metallic impurities as in Ref. [20]. A sample of unsupported Pd powder (Pd black) was prepared by a similar methodology of the Pd/C electrocatalysts. Further details are given in the [Supplementary Material](#).

The amount of Pd anchored on carbon was evaluated by means of Thermogravimetric (TG) analysis. X-Ray diffraction was used to estimate the average crystallite size of the prepared Pd/C and Pd black particles, found to be 8.1 nm and 10.9 nm, respectively. Transmission Electron Microscopy (TEM) images were obtained to visualize the agglomeration of the Pd/C materials. Apparatus, TG curves, XRD profiles, and TEM images are shown in [Supplementary Material, Fig. S1](#).

Electrochemical measurements were carried out in conventional three-electrode cell. Pd/C and Pd black electrocatalysts were studied by the thin-film electrode method reported elsewhere [21]. Typically, 2.0 mg of the powder was dispersed in 4.0 mL of isopropyl alcohol in ultrasonic bath followed by deposition of aliquots of the suspension onto a mirror-finished glassy carbon electrode (5.0 mm diameter) embedded in PTFE (Teflon®). No binder (such as Nafion®) was used to avoid possible contaminants from the polymer. A Pd wire (Johnson Matthey, geometric area of  $0.256 \text{ cm}^2$ ) was also used as the working electrode to serve as comparison. A platinum wire (area  $\approx 23 \text{ cm}^2$ ) was used as the counter electrode. All potentials were measured against an Ag/AgCl ( $3 \text{ mol L}^{-1}$  in NaCl) reference electrode. Measurements were performed in  $0.1 \text{ mol L}^{-1} \text{ H}_2\text{SO}_4$  (Merck) purged with  $\text{N}_2$  (White Martins, analytical grade 5.0) during the whole experiment. Aqueous solutions were prepared with ultrapure water ( $18.2 \text{ M}\Omega \text{ cm}$ , Gehaka, model Master All). A PAR 283 potentiostat controlled by the Power Suite software was used for data acquisition. As usually done, each electrode was cycled 10 times at  $50 \text{ mV s}^{-1}$  between  $-0.21 \text{ V}$  and  $0.8 \text{ V}$  before experiments. The uncompensated solution resistance was estimated to be about 20 Ohms by the current-interruption method. Voltammetric charges were calculated by using our recent free software ADVG [22].

## Results and discussion

The cyclic voltammetric (CV) profile of the Pd/C electrocatalysts containing distinct metal-to-carbon ratios, Pd black, and Pd wire in  $0.1 \text{ mol L}^{-1} \text{ H}_2\text{SO}_4$  are shown in [Fig. 1](#). From a qualitative viewpoint, an increase in the amount of Pd loaded on carbon resulted in a CV profile exhibiting higher currents coming from the adsorption/desorption of hydrogen ( $-0.21 < E < 0.1 \text{ V}$ ), palladium oxide formation/reduction PdO processes ( $E > 0.4 \text{ V}$ ), and minor response from the carbon phase ( $0.1 < E < 0.4 \text{ V}$ ). The Pd bulk electrode ([Fig. 1f](#)) shows a substantial different behavior compared to the nano-sized Pd electrodes. Particularly with respect to the hydrogen region, a sharp increase in the cathodic current is observed (generally ascribed to the coupling of adsorption/absorption and evolution of hydrogen), along with its large anodic counterpart (oxidation of hydrogen). The latter extends towards the whole positive-going scan, superimposing that of the formation of PdO. To avoid the interference of the hydrogen oxidation currents, a CV scan with restricted potential window (from 0.2 to  $0.9 \text{ V}$ ) was used.

The first worth noting difference between the materials is the peak potential for the reduction of palladium oxide (PdO) as function of the metal loading ([Fig. 2a](#)), where a clear trend can be observed. Beginning with the value of the Pd wire of  $E_{\text{PdO}} = 0.53 \text{ V}$  (plotted as 0%), as the amount of Pd anchored on carbon is increased it is observed a decrease in the peak potential for the PdO reduction, seeming to approach the value of  $E_{\text{PdO}} = 0.42 \text{ V}$  for the Pd black sample (plotted as 100%). The potential difference among all investigated electrodes was about 110 mV, highlighting a significant shift in the PdO reduction energetics. In other words, as the amount of Pd on carbon is increased, the reduction of oxides appears to be more irreversible. The same trend is found by using different upper potential limits, such as 0.8 and  $1.0 \text{ V}$  (See, [Supplementary Material, Figs. S3 and S4](#)).

Quantitative information regarding the processes of formation and reduction of PdO and the desorption of hydrogen ( $\text{Pd-H}_{\text{desorption}}$ ) was obtained after normalization of the corresponding voltammetric charges by the electrochemical active area determined by the Pd-H formation charges (negative-going scan) assuming a normalization factor of  $205 \mu\text{C cm}^{-2}$  of Pd, as in Ref. [23]. All values are depicted in [Fig. 2b–d](#). Although such method is not recommended for bulk Pd electrodes due to the coupling of hydrogen adsorption, absorption and evolution, such procedure was already used for nano-sized Pd electrodes given that some separation among adsorption/absorption and evolution can be found [23–25]. In fact, if a slower scan rate is used (i.e.,  $10 \text{ mV s}^{-1}$  and  $5 \text{ mV s}^{-1}$ ), it seems that adsorption/absorption and evolution are indeed taking place at distinct potential window ([Fig. S5](#)).

A trend seems to exist between the PdO reduction peak and their corresponding charges ([Fig. 2b](#)): the higher the charge of the PdO reduction, the lower the reduction peak potential. Consequently, the correlation suggests stronger palladium-oxygen interactions as the amount of PdO increases. The PdO formation and reduction charges also exhibited a clear dependence on the amount of Pd loaded on the carbon support, as shown in [Fig. 2c](#). Taking the Pd wire as the reference

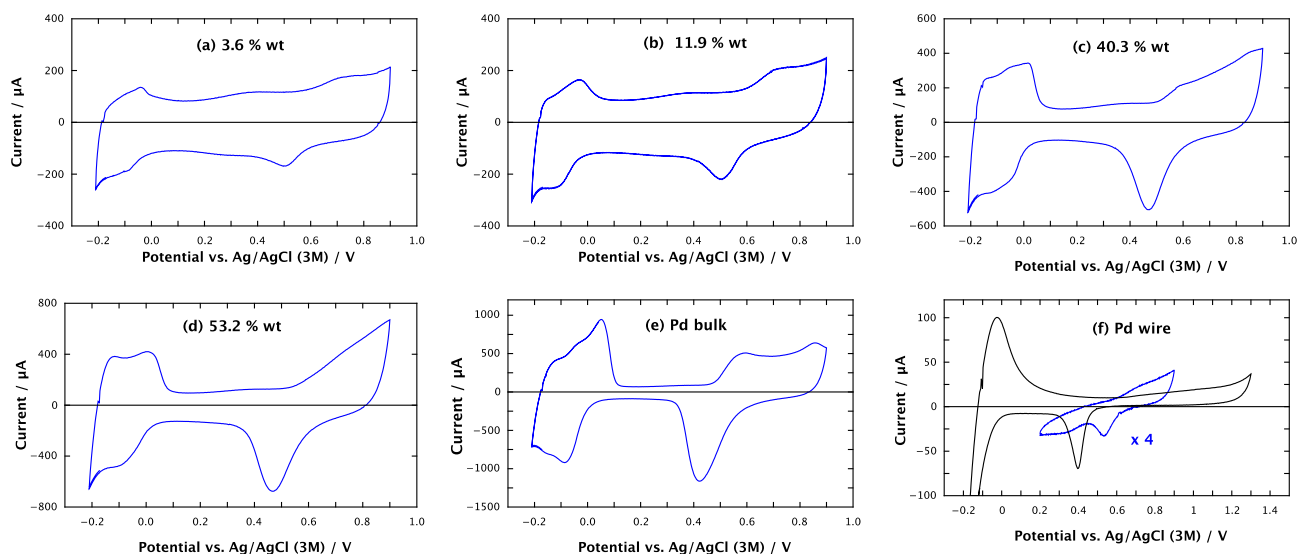


**Fig. 1** – Cyclic voltammograms obtained for Pd/C electrocatalysts containing distinct amounts of Pd loaded on carbon, Pd black and Pd wire as indicated. Scan rate =  $50 \text{ mV s}^{-1}$ ,  $0.1 \text{ mol L}^{-1} \text{ H}_2\text{SO}_4$ , room temperature ( $22^\circ \text{C}$ ). Currents for Pd wire obtained between 0.2 V and 0.9 V were multiplied by 4 (as indicated).

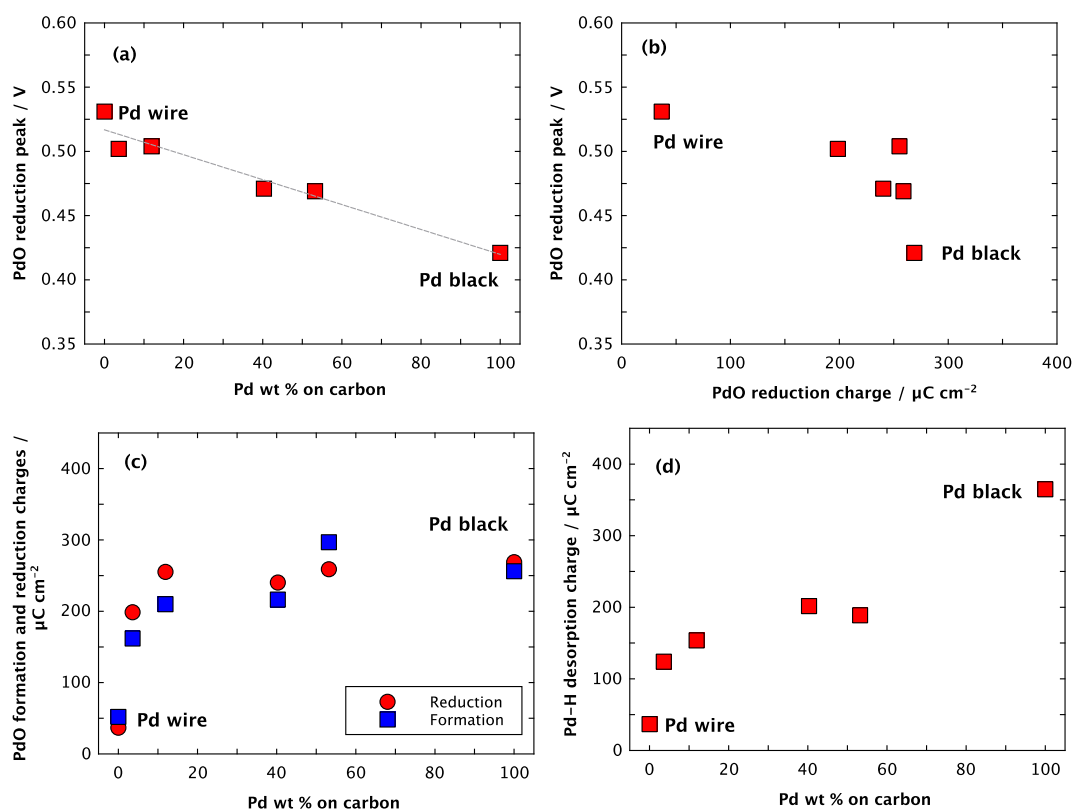


**Fig. 2** – Metal loading effects on Pd/C: (a) The peak potential for the reduction of PdO as function of the metal loading; (b) the PdO reduction peak potential as function of the PdO formation charge; (c) Charges involved in the process of PdO formation and reduction as function of the metal loading; (d) charges involved in the process of hydrogen desorption as function of the metal loading.

point, the charges initially increases and then approaches the value of  $\approx 270 \mu\text{C cm}^{-2}$  exhibited for the Pd black sample. The large difference in the charges of Pd black and Pd wire is likely caused by a higher amount of surface defects and

uncoordinated atoms in the former, due to size effects, which is known to bind oxygen more strongly [26]. The charges involved in desorption of hydrogen (Fig. 2d) also showed an increase with the metal loading but significant lower to that of

obtained for the Pd black electrode. The bulk Pd sample (Pd wire) was not included in the plot since it was one order of magnitude higher (about  $1780 \mu\text{C cm}^{-2}$ ) than those observed for the nanostructure Pd samples.

Given no similar study is available for Pd/C, a comparison will be made with results obtained for Pt/C reported on literature [17,27,28]. The most striking fact is that the observed trends for Pd/C shown in Fig. 2a are the opposite to that of found for Pt/C electrocatalysts, where a decrease in the overpotential for the reduction of PtOH is observed as the metal content is increased [27–29], and an invariant behavior of the hydrogen desorption profile (charge) with the metal loading is found [17]. For Pt/C, the alteration of the adsorptive properties observed as the Pt content on carbon is increased was explained by a change in the potential drop across the electrode/electrolyte interface caused by a decrease in the edge-to-edge distance of adjacent particles [27,28]. Given that Pd/C and Pt/C behaves differently it is clear that metal loading effects are far from being understood and requires further investigation, specially in the context of Fuel Cells.

## Summary

To the best of our knowledge, we showed for the first time that the electrochemical behavior of Pd/C electrocatalysts in  $0.1 \text{ mol L}^{-1} \text{ H}_2\text{SO}_4$  clearly depends on the amount of Pd anchored in the carbon support. Our major findings can be summarized as follow: (i) the energetics of the PdO formation/reduction is affected by the amount of Pd in the support, exhibiting higher overpotential for PdO reduction as the Pd content is increased, and; (ii) the charges related to the formation/reduction of PdO and of the Pd–H desorption increases with the metal loading. Consequently, metal-loading effects has to be taken into account when designing Pd-based Fuel Cells electrocatalysts.

## Acknowledgements

Prof. E.G. Ciapina thanks CNPq (project # 476690/2013-7) and PROPE/UNESP for financial support. Mr. L. B. Viana and Ms. R. M. I. S. Santos acknowledge PROPE/UNESP and CAPES for the scholarship, respectively. Authors thank Profs. Sergio F. dos Santos, L. Rogerio O. Hein and Edson C. Botelho for XRD and TG measurements. Authors declare no conflicts of interest.

## Appendix A. Supplementary data

Supplementary data related to this article can be found at <https://doi.org/10.1016/j.ijhydene.2018.07.137>.

## REFERENCES

- [1] Antolini E. Palladium in fuel cell catalysis. *Energy Environ Sci* 2009;2:915. <https://doi.org/10.1039/b820837a>.
- [2] Bianchini C, Shen P. Palladium-based electrocatalysts for alcohol oxidation in half cells and in direct alcohol fuel cells. *Chem Rev* 2009;4183–206.
- [3] Shao M-H. Palladium-based electrocatalysts for hydrogen oxidation and oxygen reduction reactions. *J Power Sources* 2011;196:2433–44. <https://doi.org/10.1016/j.jpowsour.2010.10.093>.
- [4] Zhu Y, Khan Z, Masel RI. The behavior of palladium catalysts in direct formic acid fuel cells. *J Power Sources* 2005;139:15–20. <https://doi.org/10.1016/j.jpowsour.2004.06.054>.
- [5] Zhou WP, Lewera A, Larsen R, Masel RI, Bagus PS, Wieckowski A. Size effects in electronic and catalytic properties of unsupported palladium nanoparticles in electrooxidation of formic acid. *J Phys Chem B* 2006;110:13393–8. <https://doi.org/10.1021/jp061690h>.
- [6] Ju W, Valiollahi R, Ojani R, Schneider O, Stimming U. The electrooxidation of formic acid on Pd nanoparticles: an investigation of size-dependent performance. *Electrocatalysis* 2016;7:149–58. <https://doi.org/10.1007/s12678-015-0293-7>.
- [7] Liu J, Ye J, Xu C, Jiang SP, Tong Y. Kinetics of ethanol electrooxidation at Pd electrodeposited on Ti. *Electrochem Commun* 2007;9:2334–9. <https://doi.org/10.1016/j.elecom.2007.06.036>.
- [8] Obradović MD, Stanić ZM, Lačnjevac UČ, Radmilović VV, Gavrilović-Wohlmuther A, Radmilović VR, et al. Electrochemical oxidation of ethanol on palladium-nickel nanocatalyst in alkaline media. *Appl Catal B Environ* 2016;189:110–8. <https://doi.org/10.1016/j.apcatb.2016.02.039>.
- [9] Moraes LPR, Matos BR, Radtke C, Santiago EI, Fonseca FC, Amico SC, et al. Synthesis and performance of palladium-based electrocatalysts in alkaline direct ethanol fuel cell. *Int J Hydrogen Energy* 2016;41:6457–68. <https://doi.org/10.1016/j.ijhydene.2016.02.150>.
- [10] Lima FHB, Zhang J, Shao M-H, Sasaki K, Vukmirovic MB, Ticianelli E a, et al. Catalytic activity-d-band center correlation for the  $\text{O}_2$  reduction reaction on platinum in alkaline solutions. *J Phys Chem B* 2007;111:404–10.
- [11] Shao M-H, Huang T, Liu P, Zhang J, Sasaki K, Vukmirovic MB, et al. Palladium monolayer and palladium alloy electrocatalysts for oxygen reduction. *Langmuir* 2006;22:10409–15. <https://doi.org/10.1021/la0610553>.
- [12] Zhu S, Hu X, Shao M-H. Impacts of anions on the oxygen reduction reaction kinetics on platinum and palladium surfaces in alkaline solutions. *Phys Chem Chem Phys* 2017;19:7631–41. <https://doi.org/10.1039/C7CP00404D>.
- [13] Mayrhofer KJJ, Bliznac BB, Arenz M, Stamenkovic VR, Ross PN, Markovic NM. The impact of geometric and surface electronic properties of Pt-catalysts on the particle size effect in electrocatalysis. *J Phys Chem B* 2005;109:14433–40. <https://doi.org/10.1021/jp051735z>.
- [14] Maillard F, Schreier S, Hanzlik M, Savinova ER, Weinkauff S, Stimming U. Influence of particle agglomeration on the catalytic activity of carbon-supported Pt nanoparticles in CO monolayer oxidation. *Phys Chem Chem Phys* 2005;7:385–93. <https://doi.org/10.1039/b411377b>.
- [15] Solla-Gullón J, Rodríguez P, Herrero E, Aldaz A, Feliu JM. Surface characterization of platinum electrodes. *Phys Chem Chem Phys* 2008;10:1359–73. <https://doi.org/10.1039/b709809j>.
- [16] Solla-Gullón J, Garnier E, Feliu JM, Leoni M, Leonardi A, Scardi P. Structure and morphology of shape-controlled Pd nanocrystals. *J Appl Crystallogr* 2015;48:1534–42. <https://doi.org/10.1107/S1600576715015964>.
- [17] López-Cudero A, Solla-Gullón J, Herrero E, Aldaz A, Feliu JM. CO electrooxidation on carbon supported platinum nanoparticles: effect of aggregation. *J Electroanal Chem*

- 2010;644:117–26. <https://doi.org/10.1016/j.jelechem.2009.06.016>.
- [18] Ciapina EG, Santos SF, Gonzalez ER. The electrooxidation of carbon monoxide on unsupported Pt agglomerates. *J Electroanal Chem* 2010;644:132–43. <https://doi.org/10.1016/j.jelechem.2009.09.022>.
- [19] Pasqualetti AM, Olu P, Chatenet M, Lima FHB. Borohydride electrooxidation on carbon-supported noble metal nanoparticles: insights into hydrogen and hydroxyborane formation. 2015. <https://doi.org/10.1021/acscatal.5b00107>.
- [20] Jirkovsky JS, Halasa M, Schiffrin DJ. Kinetics of electrocatalytic reduction of oxygen and hydrogen peroxide on dispersed gold nanoparticles. *Phys Chem Chem Phys* 2010;12:8042–52. <https://doi.org/10.1039/c002416c>.
- [21] Ciapina EG, Santos SF, Gonzalez ER. The electro-oxidation of carbon monoxide and ethanol on supported Pt nanoparticles: the influence of the support and catalyst microstructure. *J Solid State Electrochem* 2013;17:1831–42. <https://doi.org/10.1007/s10008-013-2120-5>.
- [22] Viana LB, Ciapina EG. Free software for the determination of the real surface area of fuel cells electrocatalysts abstract. 2016. <https://doi.org/10.13140/RG.2.2.30813.61923>.
- [23] Durst J, Simon C, Hasche F, Gasteiger HA. Hydrogen oxidation and evolution reaction kinetics on carbon supported Pt, Ir, Rh, and Pd electrocatalysts in acidic media. *J Electrochem Soc* 2014;162:F190–203. <https://doi.org/10.1149/2.0981501jes>.
- [24] Shao M-H, Odell JH, Choi S, Xia Y. Electrochemical surface area measurements of platinum- and palladium-based nanoparticles. *Electrochem Commun* 2013;31:46–8. <https://doi.org/10.1016/j.elecom.2013.03.011>.
- [25] Zalineeveva A, Baranton S, Coutanceau C, Jerkiewicz G. Electrochemical behavior of unsupported shaped palladium nanoparticles. *Langmuir* 2015;31:1605–9. <https://doi.org/10.1021/la5025229>.
- [26] Han BC, Miranda CR, Ceder G. Effect of particle size and surface structure on adsorption of O and OH on platinum nanoparticles: a first-principles study. *Phys Rev B Condens Matter* 2008;77:1–9. <https://doi.org/10.1103/PhysRevB.77.075410>.
- [27] Speder J, Altmann L, Bäumer M, Kirkensgaard JJK, Mortensen K, Arenz M. The particle proximity effect: from model to high surface area fuel cell catalysts. *RSC Adv* 2014;4:14971. <https://doi.org/10.1039/c4ra00261j>.
- [28] Nesselberger M, Roefzaad M, Hamou RF, Biedermann PU, Schweinberger FF, Kunz S, et al. The effect of particle proximity on the oxygen reduction rate of size-selected platinum clusters. *Nat Mater* 2013;12:919–24. <https://doi.org/10.1038/nmat3712>.
- [29] Taylor S, Fabbri E, Levecque P, Schmidt TJ, Conrad O. The effect of platinum loading and surface morphology on oxygen reduction activity. *Electrocatalysis* 2016;7:287–96. <https://doi.org/10.1007/s12678-016-0304-3>.